Zitierweise: Angew. Chem. Int. Ed. 2024, e202412759
doi.org/10.1002/anie.202412759

Metal Halides

Antiferromagnetic Ordering in A One-Dimensional Organic Copper Chloride Hybrid Insulator

Md Sazedul Islam, Andrew Comstock, Zhenqi Hua, Puja Thapa, Yufang He, Azza Ben-Akacha, He Liu, Tarannuma Ferdous Manny, Jarek Viera, Xinsong Lin, Bin Ouyang, Peng Xiong,* Dali Sun,* and Biwu Ma**

Abstract: Low dimensional (LD) organic metal halide hybrids (OMHHs) have recently emerged as new generation functional materials with exceptional structural and property tunability. Despite the remarkable advances in the development of LD OMHHs, optical properties have been the major functionality extensively investigated for most of LD OMHHs developed to date, while other properties, such as magnetic and electronic properties, remain significantly under-explored. Here, we report for the first time the characterization of the magnetic and electronic properties of a 1D OMHH, organic-copper (II) chloride hybrid $(C_8H_{22}N_2)Cu_2Cl_6$. Owing to the antiferromagnetic coupling between Cu atoms through chloride bridges in 1D $[Cu_2Cl_6^{2-}]_\infty$ chains, $(C_8H_{22}N_2)Cu_2Cl_6$ is found to exhibit antiferromagnetic ordering with a Néel temperature of 24 K. The two-terminal (2T) electrical measurement on a $(C_8H_{22}N_2)Cu_2Cl_6$ single crystal reveals its insulating nature. This work shows the potential of LD OMHHs as a highly tunable quantum material platform for spintronics.

Magnetic materials with controllable dimensionality have recently gained tremendous attention with potential applications in emerging technologies such as spintronics and quantum computing, as reduced dimensionality and size effect of the materials can significantly influence their spin arrangement.[1] On the other hand, graphene and other nonmagnetic two dimensional (2D) inorganic layered materials have been studied extensively for their superior spin dependent properties, e.g., ultra-long spin relaxation time/length, tunable spin-orbit coupling, and various emergent quantum spin effects.[2] Integrating the magnetic and nonmagnetic 2D materials, spintronic devices such as spin valves, spin transistors, and spin logic switches have been fabricated, producing many intriguing results.[3] Inspired by the successes of utilizing 2D layered materials in spintronics, there is growing interest in the spin dependent properties in 1D materials. Notably examples include recent observation of unique anisotropic spinon spin current along the chains in Sr_2CuO_3,[4] and spin-dependent charge transport in (R/S-MBA) $PbBr_3$.[5]

Owing to robust and readily accessible magnetic order and spin polarization, ferromagnetic materials have been widely utilized in spintronics as spin sources and detectors. More recently, as the research advances in this field, antiferromagnets, which were previously described as "interesting but useless" by Louis Néel, have attracted growing interest as a material for next generation information processing and storage devices.[6] The unique properties of antiferromagnets like immunity to external magnetic perturbation and absence of stray fields make them particularly attractive for spintronics. Recently, a host of insulating antiferromagnets, including hematite (α-Fe_2O_3),[7] nickel oxide (NiO),[8] and chromium thiophosphate ($CrPS_4$),[9] have been found to transport spin polarization efficiently via antiferromagnetic magnons over micrometer distances without any charge transport, thus producing no power dissipation. However, most of these insulating antiferromagnetic materials are inorganics, which in thin film forms often suffer from disadvantages like agglomeration due to high surface energy, poor processability and often require high temperature synthesis.[10]

Organic metal halide hybrids (OMHHs) are an emerging class of hybrid materials, of which the dimensionality at the molecular level can be finely controlled by choosing appropriate organic cations and metal halides for crystal growth.[11] While numerous low dimensional OMHHs, from 2D to 1D, and 0D, have been developed with their optical properties extensively studied, their magnetic and electronic properties remain significantly under-explored. Thus far, there have been a few reports on 2D OMHHs

[*] M. S. Islam, Dr. Y. He, Dr. A. Ben-Akacha, Dr. H. Liu, T. F. Manny, J. Viera, Dr. X. Lin, Prof. Dr. B. Ouyang, Prof. Dr. B. Ma
Department of Chemistry and Biochemistry
Florida State University
Tallahassee, Florida 32306, United States
E-mail: bouyang@fsu.edu
bma@fsu.edu

A. Comstock, P. Thapa, Prof. Dr. D. Sun
Department of Physics
North Carolina State University
Raleigh, North Carolina 27695, United States
E-mail: dsun4@ncsu.edu

Z. Hua, Prof. Dr. P. Xiong
Department of Physics
Florida State University
Tallahassee, Florida 32306, United States
E-mail: pxiong@fsu.edu

showing ferromagnetic, antiferromagnetic, paramagnetic, or no magnetic ordering at all,[12] Investigating the magnetic properties of OMHHs with 1D and 0D structures, containing various types of organic cations (insulating or semiconducting) and metal halide configurations (chains, ribbons, ladders, clusters, dimers with distinct corner, edge, or face-sharing polyhedra), are of great interest. Moreover, this structural diversity along with tunability makes this class of material a model system to investigate low dimensional quantum magnetism. Phenomena e.g., the cooperative behaviors of spin dimers, quantum phase transitions and associated changes in the ground state properties or the formation of gapped or gapless excitations in spin chains and ladders[13] can be better understood by studying OMHHs as it offers fine tuning of the arrangement of paramagnetic centers within the 0D and 1D structures.

Here, we report the synthesis and characterization of a unique 1D organic-copper (II) chloride hybrid $(C_8H_{22}N_2)Cu_2Cl_6$, in which edge shared square pyramidal $CuCl_5^{3-}$ co-crystalized with the organic cation $C_8H_{22}N_2^{2+}$ to form a zigzag 1D chain structure at the molecular level. The 1D $[Cu_2Cl_6^{2-}]_\infty$ chains are isolated by diamagnetic $C_8H_{22}N_2^{2+}$ moieties that eliminates any inter-chain magnetic coupling. As a result, the magnetic properties of 1D $[Cu_2Cl_6^{2-}]_\infty$ chains dominate throughout the crystals. Antiferromagnetic ordering was observed in this 1D OMHH due to coupling between adjacent Cu atoms through chloride bridges in $[Cu_2Cl_6^{2-}]_\infty$ chains. Two-terminal current–voltage (I–V) measurements were performed on individual rod-shaped $(C_8H_{22}N_2)Cu_2Cl_6$ single crystal, which manifest in hysteretic I–V curves of resistance on the order of 10 GΩ.

$(C_8H_{22}N_2)Cu_2Cl_6$ single crystals were synthesized by simple solvent evaporation, which involved evaporation of water at room temperature from a precursor solution containing N,N′-Dimethyl-1,6-hexanediamine ($C_8H_{20}N_2$) and copper (II) chloride ($CuCl_2$) (see Supporting Information for the details of synthesis). The dark red colored and rod shaped $(C_8H_{22}N_2)Cu_2Cl_6$ hybrid (Figure 1(a)) crystallizes in monoclinic space group $P2_1/n$ with $a = 6.23262$ (6) Å, $b = 12.83990(12)$ Å, $c = 10.84465(10)$ Å, and $\beta = 95.5741(9)°$, as determined by single crystal X-ray diffraction (SCXRD) (Table S1, CIF has been deposited with the CCDC 2310623).[14] The crystal structure of $(C_8H_{22}N_2)Cu_2Cl_6$, depicted in Figure 1(b), shows that the anionic metal halide chains of $[Cu_2Cl_6^{2-}]_\infty$ are completely isolated and surrounded by the organic cations $C_8H_{22}N_2^{2+}$ to form 1D structure at the molecular level. The square pyramidal $CuCl_5^{3-}$ units are connected by edge sharing to construct the individual metal halide chain in [100] direction as shown in figure 1(c). The distance between two adjacent Cu atoms along the chain is around 3.5 Å (Figure 1(d)). Two different Cu–Cl–Cu bond angles are observed in the edge sharing of $CuCl_5^{3-}$ square pyramids. The angle between Cu1–Cl1–Cu1 is 96.438(16)°, which is slightly larger than the angle 92.118(14)° between Cu1–Cl2–Cu1. The bond length of Cu1–Cl3 is 2.2710 (4) Å, while the Cu–Cl bonds within the bridges are in the

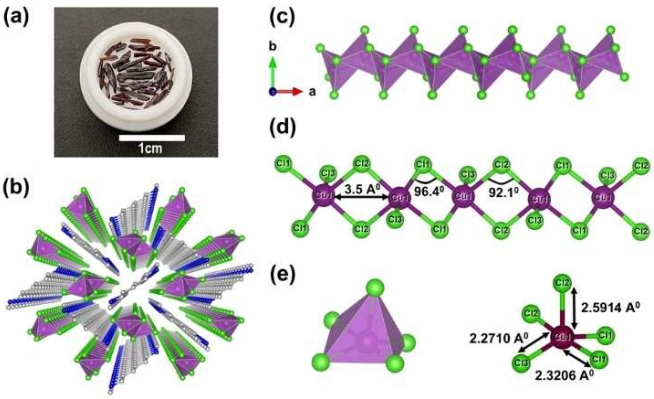

Figure 1. (a) Image of synthesized $(C_8H_{22}N_2)Cu_2Cl_6$ single crystals (b) crystal structure of $(C_8H_{22}N_2)Cu_2Cl_6$ (Light grey spheres, carbon atoms; blue spheres, nitrogen atoms; purple spheres, copper atoms; green spheres, chlorine atoms; purple polyhedrons, $[CuCl_5]^{3-}$; hydrogen atoms are hidden for clarity), (c) isolated chain of $[Cu_2Cl_6^{2-}]_\infty$ showing the arrangement of edge shared $[CuCl_5]^{3-}$ polyhedra (d) the distance between two neighboring Cu atoms in chain, and Cu–Cl–Cu bond angles (e) isolated square pyramid of $[CuCl_5]^{3-}$ in a ball and-stick-model showing the length of 3 different Cu–Cl bonds.

range of 2.2710(4) Å - 2.5914(4) Å with the longest bond length of 2.5914(4) Å for Cu1–Cl2 (Figure 1(e)) (see Supporting Information for the details of different bond lengths in Table S2 and bond angles in Table S3). Two different Cu–Cl–Cu bond angles and difference in Cu–Cl bond length led to two different $CuCl_5^{3-}$ square pyramids that occur alternatively along the chain.

The temperature dependent magnetic susceptibility data (χ) for $(C_8H_{22}N_2)Cu_2Cl_6$ were collected on single crystal from 2.5 to 300 K under an applied magnetic field of strength 0.05 T parallel to the crystallographic *a*-axis. The hybrid shows paramagnetic behavior at higher temperatures, reaching an apex at 24 K as the temperature decreases, followed by a sharp drop in susceptibility below the transition temperature, indicating antiferromagnetic ordering in the material (Figure 2). However, an upturn around 3 K indicates that there is a Curie tail due to the presence of paramagnetic impurities. The magnetization data collected at 0.05 T and 7 T are plotted in Figure S1(a) and (b), which are also consistent with the antiferromagnetic nature of the magnetic ordering in the hybrid.

As shown in Figure 2, χ^{-1} vs T plot exhibits approximate linear behavior above the transition temperature. Fitting the straight line to the Curie–Weiss equation, $\chi = \frac{C}{T-\theta}$, (where, χ is the magnetic susceptibility, C is the Curie constant and θ is the Curie–Weiss temperature) yields an effective magnetic moment (μ_{eff}) of 2.06 μ_B per Cu^{2+} and θ of −49.8 K. Although the observed μ_{eff} is slightly higher than the expected value for Cu^{2+} ($\mu_{eff} = 1.73\ \mu_B$), it is well within the range (1.7–2.2 μ_B)[15] of experimental values observed for other Cu^{2+} based materials. Magnetization vs field data was measured below ordering temperature at 5 K and is shown in Figure S1(c). No hysteresis was observed in the magnetization data and the magnetic moment does not reach saturation even at a field of 7 T,

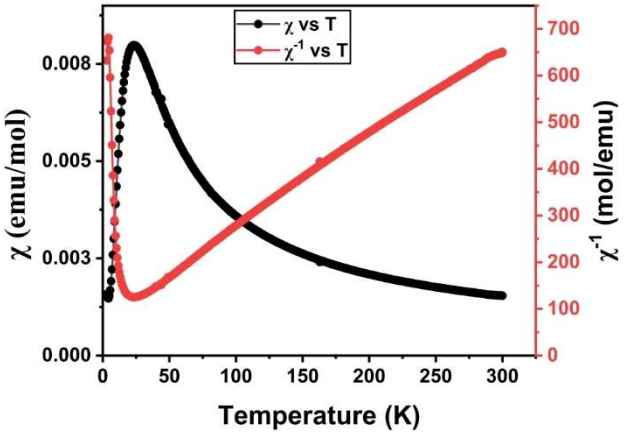

Figure 2. Temperature-dependence of magnetic susceptibility (χ) and inverse magnetic susceptibility (χ^{-1}) measured under an applied field of 0.05 T along the crystallographic a-axis on a single crystal of $(C_8H_{22}N_2)Cu_2Cl_6$.

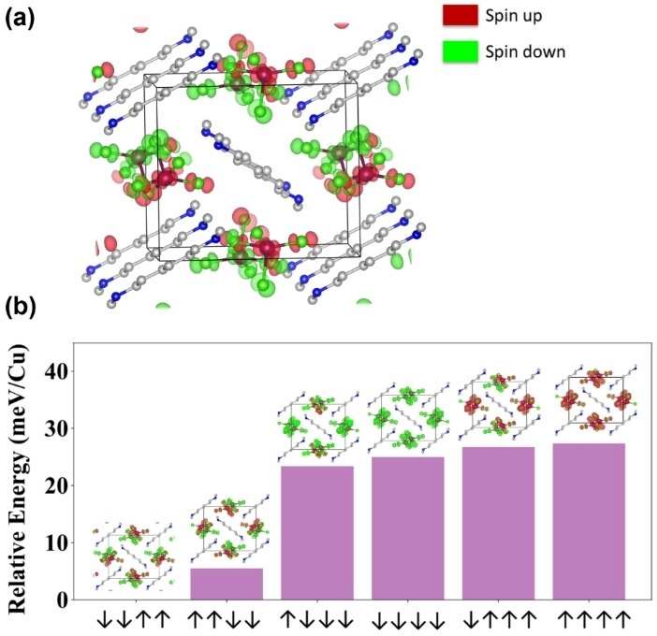

Figure 3. (a) The calculated spin density of isolated $[Cu_2Cl_6^{2-}]_\infty$ chains in $(C_8H_{22}N_2)Cu_2Cl_6$ hybrid. (b) the relative energy of selected magnetic ordering of 4 Cu atoms in $(C_8H_{22}N_2)Cu_2Cl_6$. The lowest energy configuration is set as zero energy (reference), while different antiferromagnetic and ferromagnetic states are selected to compare with the lowest energy configuration.

which is in good agreement with the antiferromagnetic nature of the magnetic ordering. No significant differences were observed in temperature and field dependent magnetization measured with the applied fields parallel and perpendicular to the a-axis (Figure S2). All the observed magnetic properties are consistent with a picture of antiferromagnetic ordering of the Cu^{2+} moments along the 1D $[Cu_2Cl_6^{2-}]_\infty$ chains, which is supported by DFT calculations below. However, the specific microscopic magnetic moment arrangement needs to be elucidated via other probes.

In order to understand the spin arrangement i.e., the origin of antiferromagnetic ordering in $(C_8H_{22}N_2)Cu_2Cl_6$ hybrid, the spin density of the isolated $[Cu_2Cl_6^{2-}]_\infty$ chains were calculated and shown in (Figure 3). All possible magnetic orderings within the unit cell of $(C_8H_{22}N_2)Cu_2Cl_6$ have been enumerated to produce DFT energies. Given that there are 4 Cu atoms in the unit cell (Figure S3(a)), the enumeration yields 16 different configurations. After DFT structure optimization, it is found that the lowest energy structure contains Cu atoms with spins oriented anti-parallel to each other within the chain leading to intra-chain antiferromagnetic ordering (Figure 3(a)). The superexchange pathway, Cu–$(Cl)_2$–Cu bichloro-bridging is responsible for this arrangement of spins. The spin arrangement along the chain is provided in Supporting Information (Figure S3(b)). Using the lowest energy structure as the reference state, six representative magnetic orderings are demonstrated in Figure 3(b), while the complete energetics are tabulated in Table S4.

Spin transport is a key process in spintronics; to understand the possible relevant pathways of spin transport in the material, i.e., diffusion of electrons in conductive materials or magnon mediated transport in magnetic insulators, it is necessary to study the electrical conductivity of the material. To assess the electrical conductivity of this hybrid, electrical contacts were made on individual rod-shaped single crystals of $(C_8H_{22}N_2)Cu_2Cl_6$ by using silver paint and Pt wire. The measurement was carried out under ambient conditions. The current–voltage (I–V) loops were measured with a sequence of instrument-controlled bias voltage V_{bias} applied from 10 V→−10 V→10 V in steps of 1 V. A symmetric current–voltage hysteresis is observed with a current of 1.16 nA at 10 V and −1.16 nA at −10 V (Figure 4).

The I–V characteristics including the hysteresis observed in 1D $(C_8H_{22}N_2)Cu_2Cl_6$ are qualitatively consistent with our previously published results in 1D (R-α-MBA)PbI_3 OMHHs,[16] where we demonstrated that the I–V hysteresis originates from intrinsic reversible ion migration characterized by a well-defined dynamic. We also showed that although the ionic migration is responsible for the hysteresis in the I–V observed in OMHHs, the linear section corresponds to the electronic current. Moreover, in the steady states, the ionic conductance is negligible in comparison to the electronic conductance, thus the sample resistance is essentially the electronic resistance (R) which can be determined by the formula I = V/R. Thus, the electrical resistance of the 1D $(C_8H_{22}N_2)Cu_2Cl_6$ hybrid was determined by taking the inverse of the slope of the linear section (specified in Figure S4) of the I–V and found to be around 9.1 GΩ. This resistance is more than an order of magnitude higher than that previously reported in 1D (R-α-MBA)PbI_3 OMHHs where the 2 T resistance was about 0.6 GΩ.[16] The higher resistance in 1D $(C_8H_{22}N_2)Cu_2Cl_6$ is likely due to the presence of linear chain organic $(C_8H_{22}N_2)^{2+}$ with no conjugation that prevents the band formation. This again

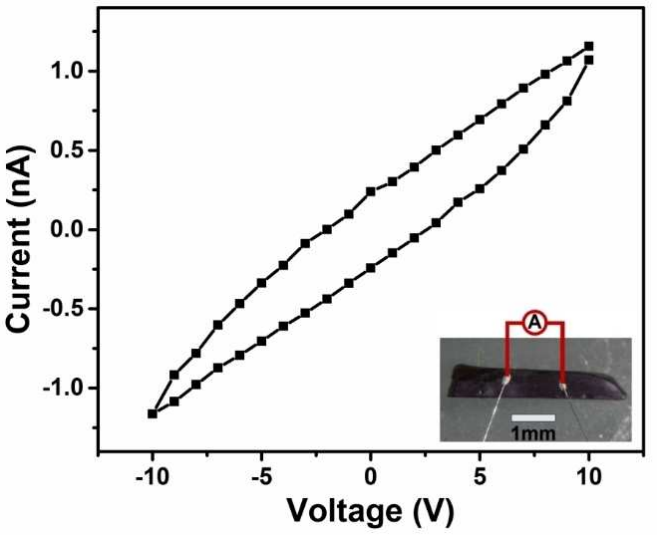

Figure 4. Full loop I–V measurements taken with applied voltage (V_{bias}) from −10 V→10 V. Inset: optical image of a wired crystal where the Pt wires are connected to the crystal by using silver paint and a schematic of the measurement setup.

shows the exceptional tunability of the optoelectronic properties of OMHHs. The (I–V) loops were also measured with two other bias voltages of −5 V→5 V and −1 V→1 V which produced similar I–V hysteresis curves and resistances of 10.3 GΩ and 11.2 GΩ respectively (Figure S4).

In summary, we have synthesized and characterized an insulating 1D OMHH, $(C_8H_{22}N_2)Cu_2Cl_6$, that shows antiferromagnetic ordering at 24 K. The presence of antiferromagnetic ordering is attributed to the antiferromagnetic coupling between adjacent Cu atoms along the chain through bichloride bridging, while the linear chain organic cations surrounding individual metal halide chains are responsible for the insulating nature of this 1D OMHH. This 1D organic-copper (II) chloride hybrid $(C_8H_{22}N_2)Cu_2Cl_6$ expands the family of electrically insulating antiferromagnetic materials for spintronics, where long-distance spin transport without dissipation due to charge transport is a primary objective. Device integration to investigate the transport of magnon spins in this 1D $(C_8H_{22}N_2)Cu_2Cl_6$ is currently underway.

Supporting Information

The authors have cited additional references within the Supporting Information.[15,17–20]

Acknowledgements

The authors acknowledge the funding support from the National Science Foundation (NSF) (DMR-2204466 (PI: Ma), DMR-1905843 (PI: Xiong), DMR-2143642 (PI: Sun), and DMR-2325147 (PI: Xiong)). Ma and Xiong also thank FSU for the Seed Grant program. Ouyang acknowledges the startup funding support from FSU. This work made use of the Rigaku Synergy-S single-crystal X-ray diffractometer that was acquired through the NSF MRI program (CHE-1828362). The Computational resources were provided by the Advanced Cyberinfrastructure Coordination Ecosystem: Services & Support (ACCESS), the National Energy Research Scientific Computing Center (NERSC), a DOE Office of Science User Facility supported by the Office of Science and the U.S. Department of Energy under contract no. DE-AC02-05CH11231 and Research Computing Center (RCC) at FSU.

Conflict of Interest

The authors declare no conflict of interest.

Data Availability Statement

The data that support the findings of this study are available from the corresponding author upon reasonable request.

Keywords: organic metal halide hybrid · one-dimensional · antiferromagnetic insulator · bichloride bridging · spin density

[1] V. P. Ningrum, B. Liu, W. Wang, Y. Yin, Y. Cao, C. Zha, H. Xie, X. Jiang, Y. Sun, S. Qin, *Research* **2020**.
[2] Y. Liu, C. Zeng, J. Zhong, J. Ding, Z. M. Wang, Z. Liu, *Nano-Micro Lett.* **2020**, *12*, 1–26.
[3] E. C. Ahn, *NPJ 2D Mater. Appl.* **2020**, *4*, 17.
[4] D. Hirobe, M. Sato, T. Kawamata, Y. Shiomi, K. I. Uchida, R. Iguchi, Y. Koike, S. Maekawa, E. Saitoh, *Nat. Phys.* **2017**, *13*, 30–34.
[5] Y. Lu, Q. Wang, R. Chen, L. Qiao, F. Zhou, X. Yang, D. Wang, H. Cao, W. He, F. Pan, *Adv. Funct. Mater.* **2021**, *31*, 2104605.
[6] D. Xiong, Y. Jiang, K. Shi, A. Du, Y. Yao, Z. Guo, D. Zhu, K. Cao, S. Peng, W. Cai, *Fundam. Res.* **2022**, *2*, 522–534.
[7] J. Han, P. Zhang, Z. Bi, Y. Fan, T. S. Safi, J. Xiang, J. Finley, L. Fu, R. Cheng, L. Liu, *Nat. Nanotechnol.* **2020**, *15*, 563–568.
[8] H. Wang, C. Du, P. C. Hammel, F. Yang, *Phys. Rev. Lett.* **2014**, *113*, 097202.
[9] D. K. de Wal, A. Iwens, T. Liu, P. Tang, G. E. Bauer, B. J. van Wees, *Phys. Rev. B* **2023**, *107*, L180403.
[10] J. Yuan, Y. Xu, A. H. Müller, *Chem. Soc. Rev.* **2011**, *40*, 640–655.
[11] C. Zhou, H. Lin, S. Lee, M. Chaaban, B. Ma, *Mater. Res. Lett.* **2018**, *6*, 552–569.
[12] a) Y. Asensio, S. Marras, D. Spirito, M. Gobbi, M. Ipatov, F. Casanova, A. Mateo-Alonso, L. E. Hueso, B. Martín-García, *Adv. Funct. Mater.* **2022**, *32*, 2207988; b) P. Vishnoi, J. L. Zuo, X. Li, D. C. Binwal, K. E. Wyckoff, L. Mao, L. Kautzsch, G. Wu, S. D. Wilson, M. G. Kanatzidis, *J. Am. Chem. Soc.* **2022**, *144*, 6661–6666.
[13] A. Vasiliev, O. Volkova, E. Zvereva, M. Markina, *NPJ Quantum Mater.* **2018**, *3*, 18.
[14] Deposition numbers 2310623 contain the supplementary crystallographic data for this paper. These data are provided free of charge by the joint Cambridge Crystallographic Data Centre and Fachinformationszentrum Karlsruhe Access Structures service.

[15] S. Mugiraneza, A. M. Hallas, *Commun. Phys.* **2022**, *5*, 95.
[16] Z. Hua, A. Ben-Akacha, Q. He, T. Liu, G. Boyce, M. van Deventer, X. Lin, H. Gao, B. Ma, P. Xiong, *ACS Energy Lett.* **2022**, *7*, 3753–3760.
[17] O. V. Dolomanov, L. J. Bourhis, R. J. Gildea, J. A. Howard, H. Puschmann, *J. Appl. Crystallogr.* **2009**, *42*, 339–341.
[18] G. M. Sheldrick, *Acta Crystallogr. Sect. C* **2015**, *71*, 3–8.
[19] J. Hafner, G. Kresse, in *Properties of Complex Inorganic Solids*, Springer **1997**, pp. 69–82.
[20] a) J. P. Perdew, K. Burke, M. Ernzerhof, *Phys. Rev. Lett.* **1996**, *77*, 3865–3868; b) G. Kresse, J. Furthmüller, *Phys. Rev. B* **1996**, *54*, 11169–11186.

Manuscript received: July 7, 2024
Accepted manuscript online: July 30, 2024
Version of record online: September 20, 2024

Zuschrift

Metal Halides

M. S. Islam, A. Comstock, Z. Hua, P. Thapa, Y. He, A. Ben-Akacha, H. Liu, T. F. Manny, J. Viera, X. Lin, B. Ouyang,* P. Xiong,* D. Sun,* B. Ma* _ **e202412759**

Antiferromagnetic Ordering in A One-Dimensional Organic Copper Chloride Hybrid Insulator

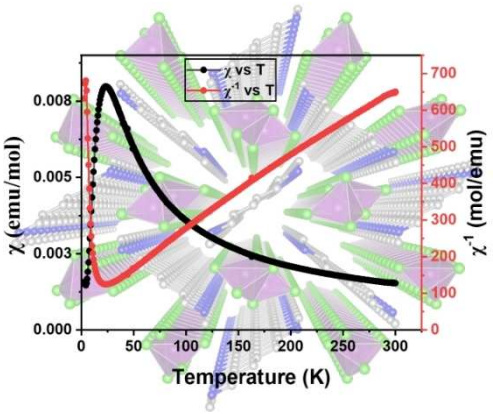

A one-dimensional (1D) organic metal halide hybrid, $(C_8H_{22}N_2)Cu_2Cl_6$, has been synthesized and characterized for the first time, which exhibits antiferromagnetic ordering with a Néel temperature of 24 K. This work paves novel pathways for developing functional low-dimensional organic metal halide hybrids for spintronics.